Original

Ultrasonographic study of hemodynamics and contrast-enhanced ultrasound in the rhesus monkey kidney

Hong WANG[1], Qipu FENG[2], Chao LI[3], Huan ZHANG[1] and Yulan PENG[1]

[1]Department of Ultrasound, West China Hospital of Sichuan University, 37 Guoxuexiang, Chengdu, 610041, P.R. China

[2]Regenerative Medicine Research Center, West China Hospital of Sichuan University, 1 keyuansilu, Chengdu, 610041, P.R. China

[3]Department of Oncology, The General Hospital of Western Theater Command PLA, 270 Rongdu Ave, Chengdu, 610083, P.R. China

Abstract: Nonhuman primates share many developmental similarities with humans. As the world has recognized the rhesus monkey as a standard experimental monkey, studies of rhesus monkey are very important and essential. The purpose of this study was to use gray-scale ultrasound, color Doppler flow imaging (CDFI), and contrast-enhanced ultrasound (CEUS) to study the ultrasound appearance of adult healthy rhesus monkey kidneys and to investigate the relationship between renal ultrasound manifestations and body weight, gender, and the left and right kidneys. Thirty adult healthy rhesus monkeys were studied in the experiments. The size of the kidney and the length and diameter of the renal artery were measured. The peak systolic velocity (PSV), end diastolic velocity (EDV), and resistance index (RI) of the renal artery and intrarenal arteries were measured by CDFI. In CEUS, the time-intensity curve (TIC) was used to obtain microvascular perfusion parameters. There were significant differences in renal size, diameter and length of the renal artery, and hemodynamics of the renal arteries between the different weight groups. In CEUS, there were significant differences in area under curve (AUC), time from peak to one half (THP), intensity peak (PI), time to peak (TTP), mean transit time (MTT), and wash-in-slope (WIS) between the different weight groups. There were no statistical differences between genders or the left and right kidneys. Our study provides valuable reference data for the studies of the kidney and indicates that CEUS can be used to evaluate renal perfusion in rhesus monkeys.

Key words: hemodynamic, renal vasculature, rhesus monkey, ultrasound

Introduction

The rhesus monkey carries significant genetic and phenotypic similarities to humans and has been recognized as a standard experimental monkey [1, 2]. Numerous studies on rhesus monkey kidneys have focused on disease models such as those for diabetic nephropathy and kidney transplantation [3–5]. With the increasing importance of animal experiments in scientific research, ultrasound (US) has been widely used in animal experiments. Various new ultrasound-related technologies have emerged, such as contrast-enhanced ultrasound (CEUS), photoacoustic imaging, and UTMD (ultrasound-targeted microbubble destruction). Studies [6] of animal models combined with US, which provide significant insights with respect to mechanisms and potential therapeutic target, have been popular in recent years. However, there are still no available reports describing the normal values for renal morphology, hemodynamics, and performance of CEUS derived by sonography in rhesus monkeys under sedation. Therefore, this study aimed to evaluate the renal morphology, normal hemodynamics of the renal

artery (RA) and intrarenal arteries (SA, segmental artery; IA, interlobar artery; AA, arcuate artery), and the performance of CEUS in the kidneys of the adult healthy rhesus monkey.

Materials and Methods

Animals

All animals (20 males and 10 females: age range, 4–6 years; weight range, 4.3–12 kg; mean weight ± SD, 6.8 ± 1.9 kg) were acquired from a government accredited experimental animal breeding and research base (Chengdu Pingan, Sichuan, China). They were housed in a large animal care facility with a constant temperature of 20°C ± 1°C and a 6 AM to 6 PM light cycle. A period of at least one month was allowed for the animals to acclimatize to the animal facility before the study. They were fed standard dry monkey food, washed apples, and water ad libitum. All animal procedures were approved by the Institutional Animal Care and Use Committee (IACUC) at West China Hospital of Sichuan University and were in accordance with the guidelines of the U.S. National Institutes of Health.

The animals were divided into two groups according to body weight: group 1, 4.3–7.0 kg (24 subjects, including 14 males and 10 females; mean weight ± SD, 6.1 ± 1.0 kg), and group 2, 7.5–12 kg (6 subjects, all of which were male; 9.8 ± 1.6 kg). The animals in group 1 were divided by gender into two groups: group 3, which was comprised of males in the 4.3–7.0 kg weight range, and group 4, which was comprised of females in the 4.3–7.0 kg weight range. All subjects were sedated by intramuscular injection of ketamine (5 mg/kg) followed by midazolam (0.2 mg/kg), and supplemented as needed throughout the experiment. The hair in a wide area over the lateral and ventral abdomen was removed with electric clippers prior to ultrasound examinations. Coupling gel was applied to the abdomen of each rhesus monkey.

Methods

All scans were performed with the subjects lying in a supine or side position and using the same sonography system (iU22, Philips Medical Systems, Royal Philips Electronics, The Netherlands). The ultrasound examinations were performed with the animal manually restrained in dorsal recumbency. In each monkey, traditional B-mode ultrasound, CDFI, and CEUS were performed on both kidneys. B-mode US was performed to scan the kidneys and renal arteries. First, a 5–12 MHz high-frequency linear transducer was used to obtain a full view of the main renal artery. The length of the main renal artery was determined by measuring the distance

from its origin to the renal hilus. The diameter of the main renal artery was measured from one intima to the other perpendicularly in systole. Ragarding the selection of ultrasound equipment for experimental use, an appropriate balance between spatial resolution and depth of ultrasound penetration has to be found. Given the limitation of the 5–12 MHz probe itself and the desire to obtain a better view in the renal ultrasonogram and renal blood perfusion by Doppler US, a curvilinear 5–1 MHz transducer was used to determine renal size and hemodynamics. Renal echos (renal cortex, renal medulla, and collecting system) and the presence of abnormalities in the kidney were observed. A longitudinal image of the kidney was used to obtain the maximum bipolar length. Width and ventral-to-dorsal height were measured at the level of the hilus. Width was measured by rotating the ultrasound head 90° to achieve a transverse view at the level of the renal hilus. All of these measurements were made using gray-scale echo mode. In CDFI, renal flow was first visualized via a color Doppler examination. Subsequently, the imaging settings, such as gain, depth, and focus, were optimized to ensure clear visualization of the renal vasculature and kidneys. These settings then remained the same throughout the experiment. Once the regions were visualized, pulsedwave recording was performed for the RA (near its aortic origin), SA (first level of the renal artery branch), IA (which crosses the medulla from the renal sinus to the corticomedullary junction), and AA (which travels across the top of the renal pyramids and gives rise to arteriae interlobulares renis). The vasculature at each level was measured three times from three different sites (cranial, middle, and caudal poles). The following indices were measured manually using the built-in calipers of the sonographic machine: peak systolic velocity (PSV), end-diastolic velocity (EDV), and resistive index (RI). All Doppler flow spectra recorded for analysis consisted of 3 to 5 consecutive similar-appearing waveforms.

In order to observe the CEUS performance of SonoVue in rhesus monkey kidneys, a 22-gauge indwelling catheter was placed in the right cubital vein, and a 3-way stop-cock was applied at the end of the catheter, with 1 branch being used for administration of the contrast agent and another for a physiologic saline flush after contrast agent administration. The 3-way stopcock was used to avoid any delay between the injection of contrast agent and saline. The mechanical index setting was 0.06 for CEUS, and adjustable parameters such as depth, gain, and focus were optimized and held constant during the study. We set an image capture time of 1 min after intravenous bolus injection of the contrast agent. The kidney of interest was centered on the screen and was imaged

in a longitudinal plane using dual-screen mode (simultaneous display of conventional B-mode and contrast-mode images). The transducer was manually positioned during each imaging procedure and was maintained in the same position during CEUS. The contrast agent, (SonoVue, Bracco SpA, Milan, Italy; 0.05 ml/kg) was injected (bolus injection over approximately 3 s), and this was followed by injection of a 1.0 ml saline bolus. The same person performed the injection in a standardized manner for all the rhesus monkeys. Two injections (right and left kidney) of SonoVue were performed for each rhesus monkey. The interval between the two injections was at least 15 min, and residual bubbles were cleared off with a flash echo technique at a high mechanical index setting.

The recordings were analyzed using specialized computer software (QLAB) for objective quantitative analysis. Three regions of interest (ROIs) were manually drawn in the renal cortex. The ROIs were similar in size and drawn at almost the same depth in every region. For each ROI, the software was used to automatically generate a smoothed time-intensity curve (TIC) using a fitting technique and related quantitative parameter values, including the rise time (RT), peak intensity (PI), mean transit time (MTT), area under the curve (AUC), wash-in slope (WIS), time from peak to one half (TPH), and time-to-peak (TTP). RT was defined as the time from injection until the peak of enhancement. PI was defined as the peak intensity of enhancement. MTT was defined as the duration of the increase in intensity until it decreased to 50% of the maximum intensity. AUC was defined as the area under the time-intensity curve. WIS was defined as the speed from the beginning of enhancement to the peak of enhancement. TPH was defined as the time needed after injection until the intensity decreased to half of the PI. TTP was defined as the interval from injection to the peak of the time-intensity curve.

Data are expressed as the mean ± SD. Statistical analysis was performed using Student's t-test and $P<0.05$ was considered statistically significant.

Results

B-mode ultrasound imaging

In our study, high-frequency ultrasonography could obtain a clear main renal artery ultrasonogram (Fig. 1). The entire renal artery could be seen in all animals. It originated from the ventral aspect of the aorta, and its path from the aorta to the hilum was slightly different among the subjects. The mean diameter and length of the RA for the rhesus monkeys in group 1 were 0.21 ± 0.06 cm and 1.91 ± 0.33 cm; the results for the rhesus
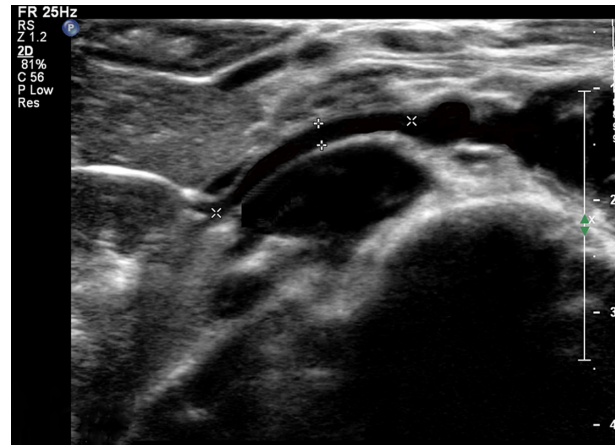

Fig. 1. High-frequency ultrasound clearly showed the shape of the renal artery from the abdominal aorta to the renal hilum. +, diameter of renal artery; ×, length of renal artery.

monkeys in group 2 were 0.24 ± 0.04 cm and 2.11 ± 0.32 cm. With the a curvilinear 5–1 MHz transducer, the shapes of the right and left kidneys resembled that of the human kidney. The left and right renal cortices were isoechoic to the spleen and liver, respectively. The renal cortex was hyperechoic relative to the medulla, and there was a distinct demarcation between the cortex and the medulla at the corticomedullary junction. The echo intensity of the collecting system was significantly higher than that of the renal parenchyma, with no obvious anechoic areas. Furthermore, no evidence of focal or diffuse abnormalities was found in the kidneys. The measurements of kidney size (length, width, and height, respectively) were 4.66 ± 0.55 cm, 2.49 ± 0.35 cm, 2.27 ± 0.50 cm for group 1 and 6.19 ± 0.30 cm, 3.06 ± 0.38 cm, 3.26 ± 0.31 cm for group 2. There were significant differences in diameter and length of the renal artery and in kidney size between the two body weight groups ($P<0.05$). There were no statistical differences between genders or between the left and right kidneys.

Doppler ultrasound

The left and right main intrarenal arteries and veins were easily visualized along their entire courses. In addition, one accessory renal artery that originated from the abdominal aorta was found in the right kidney of a male rhesus monkey. For this reason, insonation of the artery for waveform analysis was performed at its origin, where the vessel had a more consistent perpendicular relationship relative to the aorta. The intrarenal vascular distribution in the kidney is dendritic, and the location of the intrarenal vasculature was examined with color Doppler (Fig. 2).

In color flow ultrasound, the distribution of intrarenal artery blood flow is dendritic in rhesus monkeys. Spec-

tral Doppler can quantify renal hemodynamics. Blood flow velocity decreased progressively in the different intrarenal arteries as they branched off from the renal artery in the parenchyma of the kidneys. The shape of the Doppler waveforms was similar to that described for humans (Fig. 3). In Fig. 3, the normal Doppler waveform obtained for the intrarenal arteries shows a low resistance profile with continuous forward flow throughout the cardiac cycle. The results obtained for the two body groups are summarized in Table 1. There were significant differences in PSV, EDV, and RI between the two groups. These parameters were higher in the higher body weight group. The results obtained for the gender groups are summarized in Table 2. No significant differences were observed between the gender groups. There were also no statistical differences between the left and right kidneys.

CEUS performance

After the injection of SonoVue, the renal artery, cortex, medulla, and renal vein were observed in sequence. The TIC for renal perfusion in the renal cortex was an asymmetrical curve with a single-peak. It showed an obvious ascending slope, peak, and descending slope (Fig. 4). The ascending slope tended to ascend quickly and then decrease after reaching the peak. The results of the quantitative analysis for the two body weight groups are shown in Table 3. Group 2 showed higher values for PI, AUC, HPT, and WIS and longer values for TTP and MTT ($P<0.05$). Analysis of RT revealed no significant difference between group 1 and group 2. The results of the quantitative analysis for the different gender groups are shown in Table 4. No significant differences were observed between the gender groups or the left and right kidneys.
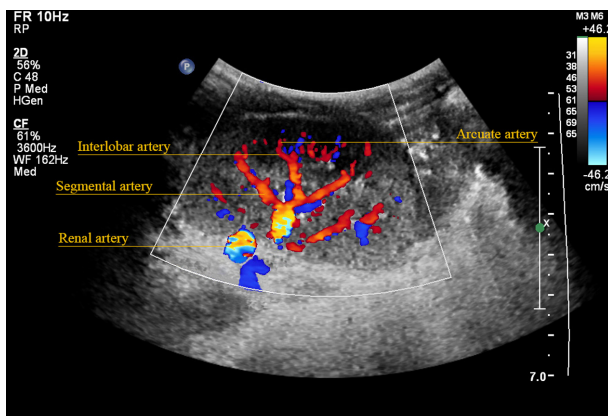

Fig. 2. Color ultrasound imaging showed that the blood vessels in the kidney of rhesus monkey are distributed like branches. This image clearly shows the dendritic structure of the renal vessels. The segmental artery is the first branch of the renal artery in the kidney. The interlobar artery is located in the corticomedullary junction. The arcuate artery passes through the apex of the renal vertebral body.
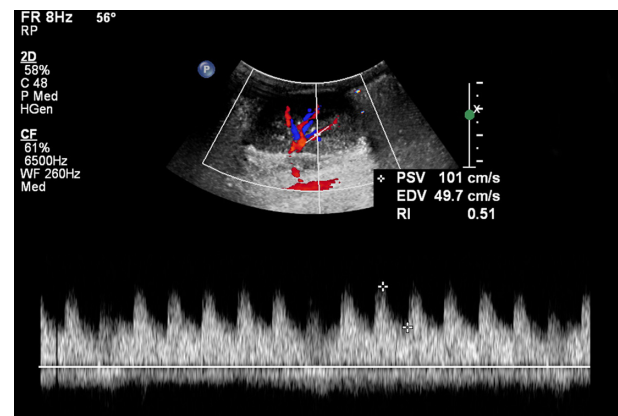

Fig. 3. Color Doppler image showing the spectral waveform morphology of the intrarenal arteries.

Table 1. Kidney hemodynamic parameters obtained from different weight groups of rhesus monkey

		PSV (cm/s)	EDV (cm/s)	RI
RA	Group 1	119.85 ± 18.99	55.44 ± 11.86	0.54 ± 0.06
	Group 2	127.0 ± 7.64	46.05 ± 5.30	0.70 ± 0.06
SA	Group 1	92.31 ± 17.87	42.49 ± 12.10	0.54 ± 0.07
	Group 2	95.15 ± 3.46	38.80 ± 12.59	0.62 ± 0.14
IA	Group 1	73.22 ± 14.23	33.81 ± 8.99	0.54 ± 0.09
	Group 2	81.43 ± 11.30	27.83 ± 2.97	0.69 ± 0.08
AA	Group 1	54.53 ± 11.60	23.81 ± 4.33	0.54 ± 0.09
	Group 2	62.78 ± 4.91	20.58 ± 4.20	0.56 ± 0.06

Group 1: weight of 4.3–7.0 kg. Group 2: weight of 7.5–12 kg. RA: renal artery; SA: segmental artery; IA; interlobar artery; AA; arcuate artery. PSV: peak systolic velocity; EDV: end-diastolic velocity; RI: resistive index.

Table 2. Kidney hemodynamic parameters obtained from different gender groups of female rhesus monkey

		PSV (cm/s)	EDV (cm/s)	RI
RA	Group 3	120.16 ± 18.62	55.40 ± 12.67	0.54 ± 0.08
	Group 4	119.53 ± 15.56	55.47 ± 11.04	0.54 ± 0.04
SA	Group 3	92.82 ± 18.11	42.41 ± 11.96	0.54 ± 0.08
	Group 4	91.79 ± 17.58	42.56 ± 12.21	0.54 ± 0.06
IA	Group 3	73.40 ± 13.88	33.57 ± 8.76	0.54 ± 0.09
	Group 4	73.03 ± 14.54	43.05 ± 9.02	0.54 ± 0.09
AA	Group 3	54.87 ± 12.89	20.01 ± 4.2	0.53 ± 0.08
	Group 4	54.38 ± 10.3	19.89 ± 8.1	0.53 ± 0.08

Group 3, males with body weights 4.3–7.0 kg; group 4, female with body weights 4.3–7.0 kg; RA, renal artery; SA, segmental artery; IA, interlobar artery; AA, arcuate artery.
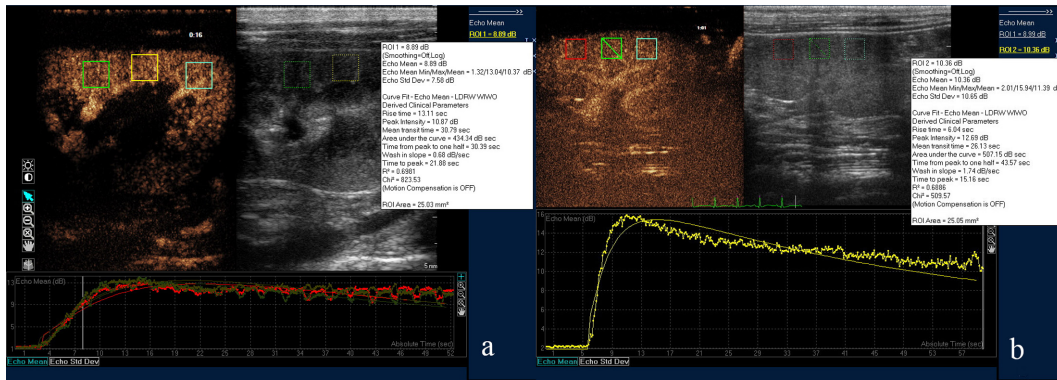
Fig. 4. (a) TIC of renal perfusion in group 1. (b) TIC of renal perfusion in group 2. (TIC, time-intensity curve.)

Table 3. The specific parameters of TIC obtained from different weight groups of rhesus monkey

	Group 1	Group 2	*P*
rise time (s)	8.45 ± 1.23	8.43 ± 1.54	>0.05
peak intensity (dB)	10.77 ± 0.7	14.06 ± 2.50	<0.05
mean transit time (s)	29.93 ± 0.82	32.34 ± 0.98	<0.05
area under the curve (dB s)	420.86 ± 31.31	582.69 ± 122.62	<0.05
time from peak to one half (s)	31.17 ± 1.84	40.84 ± 2.36	<0.05
wash in slope (dB/s)	0.77 ± 0.16	0.88 ± 0.13	<0.05
time to peak (s)	14.13 ± 2.17	17.54 ± 1.97	<0.05

Group 1, body weight of 4.3–7.0 kg; group 2, body weight of 7.5–12 kg.

Table 4. The specific parameters of TIC obtained from different gender groups of rhesus monkey

	Group 3	Group 4	*P*
rise time (s)	8.45 ± 1.43	8.44 ± 1.34	>0.05
peak intensity (dB)	10.77 ± 0.9	10.78 ± 0.4	>0.05
mean transit time (s)	29.92 ± 0.84	30.03 ± 0.43	>0.05
area under the curve (dB s)	420.98 ± 31.33	419.92 ± 43.12	>0.05
time from peak to one half (s)	31.16 ± 1.89	31.33 ± 1.34	>0.05
wash in slope (dB/s)	0.77 ± 0.15	0.76 ± 0.14	>0.05
time to peak (s)	14.13 ± 2.78	14.15 ± 2.14	>0.05

Group 3, males with body weights of 4.3–7.0 kg; group 4, females with body weights of 4.3–7.0 kg.

Discussion

At present, many studies on rhesus monkey kidney focus on animal models such as rhesus monkeys with diabetic nephropathy and kidney transplantation. However, due to the limitation of using small numbers of animals and the different purposes of observation, ultrasound plays a limited role in these studies. In this study, we investigated for the first time the usefulness of US and CEUS for in vivo imaging of kidneys, established reference values for normal renal CDFI and microvascular perfusion parameters for future studies, and discussed the effect of weight, gender, and the left and right kidney on ultrasoud performance in healthy adult rhesus monkey kidneys.

The size of the kidney, as an important content of growth index, often reflects the functional state of the kidney. In human studies, normal renal volume changes are positively correlated with renal function [7]. Hill *et al.* [8] reported that the mean kidney volume of the adult female rhesus monkey was 12 ml according to radiographic measurements and that all apparently normal adult female rhesus monkeys typically have similar sized kidneys. When we calculated the kidney volume (kidney volume=length × width × height × 0.49) in our study, the results were found to be consistent with the literature.

The renal microcirculation may be especially important in understanding renal function. In a study of renal anatomy in the rhesus monkey, Horacek *et al.* [9] provided a detailed morphological description of the microvasculature in the kidneys. However, there have been few studies on the hemodynamics of the internal renal artery. Due to the many factors that affect Doppler flow measurement of renal arteries and intrarenal arteries,

such as the instruments, measurement location, and animal anesthesia state, there are few reports on the normal reference values for the Doppler flow velocity of renal arteries and intrarenal arteries in common experimental animals. In this experiment, we investigated the usefulness of US for in vivo imaging of the kidneys and determination of renal hemodynamics and set normal reference values for future studies of adult healthy rhesus monkeys under sedation. The PSV of the renal artery was similar to that reported by Gaschen *et al.* [10] in the adult healthy cynomolgus monkey kidney. In humans, the normal main renal artery blood flow velocity is 50–100 cm/s. Our results revealed that the blood flow velocity in the renal artery of rhesus monkeys is significantly higher than that of the renal vasculature of humans. We speculated that this phenomenon may be related to heart rate, as previous studies showed that a faster the heart rate was associated with a higher blood flow velocity in the intrarenal arteries [11–13]. Of course, further work must be done to examine the effects of blood pressure and heart rate on changes in renal arterial hemodynamics. The present study also showed that the blood flow PSV values of the renal artery and intrarenal arteries increased as body weight increased.

The RI of the renal arteries is of great significance for the diagnosis and evaluation of kidney disease [14]. As there have been few studies on the application of ultrasound to the renal vasculature of rhesus monkeys, most of the reported results for RI have focused on the RA. In animal studies of RI in the renal artery, Novellas *et al.* [15] reported an average RI of 0.62 ± 0.04 in healthy cats, Carvalho *et al.* [16] reported an average RI of 0.53 ± 0.07 in healthy Persian cats, and the upper limit of RI was 0.70. In a study on the influence of the left and right kidneys on RI, Freccero *et al.* [17] reported that the renal RI value of the right kidney (0.58 ± 0.006) was higher than that of the left kidney (0.51 ± 0.006) in horses. Novellas *et al.* [15] reported an average RI of 0.62 ± 0.04 in dogs. In humans, there is no agreement on a standard RI in daily medical use or published research: previous studies used a cutoff between 0.70 and 0.80, based on the optimal cutoff in their specific population [18]. In this study, there were statistical differences in the RI values of the renal artery and intrarenal arteries between the two body weights groups. Considering the individual differences in experimental animals, the influence of body weight on the RI values of the renal artery and intrarenal arteries needs to be studied further. These results also suggest that researchers should try to select animals within a small weight range when selecting experimental animals.

CEUS has been widely studied in human kidney diseases and is effective for differentiating renal masses and diffuse kidney lesions [19, 20]. However, the use of CEUS in animal kidney disease experiments is rare. A literature review found that there were few reports on the use of CEUS in experimental animals [21–23]. Information about renal morphology and function in veterinary medicine is limited. Stock *et al.* [21] reported that lower peak enhancement and wash-in area under the curve in older cats may indicate a lower blood volume. Further studies of CEUS in the rhesus monkey kidney are needed to examine the influence of different factors, such as age, weight, and gender, and disease types on CEUS performance.

Our study, however, has many limitations. First, an appropriate balance between spatial resolution and depth of ultrasound penetration must be found when selecting ultrasound equipment for experimental use. In order to evaluate the entire monkey kidney in this study, two different frequency probes were used. A high-frequency ultrasound probe can visualize the rhesus monkey kidney and renal artery clearly. A low-frequency ultrasound probe for the kidneys can visualize the parenchyma of the kidneys and the collecting system clearly. Thus, the renal size, diameter, and length of the main renal artery can be measured accurately. Color Doppler ultrasound can display the renal artery and intrarenal arteries clearly. However, the selection of probes with different frequencies may have an impact on the experimental results. Furthermore, an analysis of previous literature regarding research on CEUS in rhesus monkey kidney [24] found that the commonly used dose of contrast agent in animal experiments is 0.05 ml/kg. Taking into consideration our experience in clinical work and animal experiments, the dose was set to 0.05 ml/kg in our CEUS study. Further study is needed to determine the optimal dose of CEUS and to examine the performance of CEUS in different diseases in the kidney of rhesus monkeys. As for the selection of the sedation method, a relatively conventional sedation method was adopted for the rhesus monkeys because this experiment mainly involved noninvasive ultrasound examinations and only required that the animals be restrained and kept quiet. The influence of the anesthesia method on the experimental results needs further study. In addition, respiratory movements, hands-on manipulation, the small sample size, and the small diameter of vasculature may affect the accuracy of experimental data. In view of the scarce literature related to the technical use of noninvasive monitoring of renal hemodynamics in rhesus monkeys, we believe that the results of the present study are interesting as they can provide insights for further research.

Conclusion

In conclusion, the present study describes for the first time the hemodynamics of the kidney in healthy adult rhesus monkeys and the performance of CEUS imaging. It also provides valuable reference data of hemodynamic parameters and microcirculatory perfusion for the studies of the kidney. In addition, the results illustrate the importance of choosing an appropriate range of body weight in animal experiments. Overall, this study suggests that ultrasound can provide information about hemodynamic parameters and microcirculatory perfusion for renal studies in rhesus monkeys.

References

1. Brichard SM, Henquin JC. The role of vanadium in the management of diabetes. Trends Pharmacol Sci. 1995; 16: 265–270. [Medline] [CrossRef]
2. Batchelder CA, Lee CC, Martinez ML, Tarantal AF. Ontogeny of the kidney and renal developmental markers in the rhesus monkey (Macaca mulatta). Anat Rec (Hoboken). 2010; 293: 1971–1983. [Medline] [CrossRef]
3. An X, Liao G, Chen Y, Luo A, Liu J, Yuan Y, et al. Intervention for early diabetic nephropathy by mesenchymal stem cells in a preclinical nonhuman primate model. Stem Cell Res Ther. 2019; 10: 363–379. [Medline] [CrossRef]
4. Thomson AW, Ezzelarab MB. Generation and functional assessment of nonhuman primate regulatory dendritic cells and their therapeutic efficacy in renal transplantation. Cell Immunol. 2020; 351: 104087–104094. [Medline] [CrossRef]
5. Ezzelarab MB, Raich-Regue D, Lu L, Zahorchak AF, Perez-Gutierrez A, Humar A, et al. Renal Allograft Survival in Nonhuman Primates Infused With Donor Antigen-Pulsed Autologous Regulatory Dendritic Cells. Am J Transplant. 2017; 17: 1476–1489. [Medline] [CrossRef]
6. Zhang Q, Yu Z, Xu Y, Zeng S, Zhang Z, Xue W, et al. Use of contrast-enhanced ultrasonography to evaluate chronic allograft nephropathy in rats and correlations between time-intensity curve parameters and allograft fibrosis. Ultrasound Med Biol. 2016; 42: 1574–1583. [Medline] [CrossRef]
7. Rodríguez LV, Spielman D, Herfkens RJ, Shortliffe LD. Magnetic resonance imaging for the evaluation of hydronephrosis, reflux and renal scarring in children. J Urol. 2001; 166: 1023–1027. [Medline] [CrossRef]
8. Hill LR, Hess KR, Stephens LC, Tinkey PT, Price RE. Comparison of kidney weight and volume to selected anatomical parameters in the adult female rhesus monkey (Macaca mulatta). J Med Primatol. 1999; 28: 67–72. [Medline] [CrossRef]
9. Horacek MJ, Earle AM, Gilmore JP. The renal microvasculature of the monkey: an anatomical investigation. J Anat. 1986; 148: 205–231. [Medline]
10. Gaschen L, Menninger K, Schuurman HJ. Ultrasonography of the normal kidney in the cynomolgus monkey (Macaca fascicularis): morphologic and Doppler findings. J Med Primatol. 2000; 29: 76–84. [Medline] [CrossRef]
11. Deane C. Doppler and color Doppler ultrasonography in renal transplants: chronic rejection. J Clin Ultrasound. 1992; 20: 539–544. [Medline] [CrossRef]
12. Kienzle MG, Ferguson DW, Birkett CL, Myers GA, Berg WJ, Mariano DJ. Clinical, hemodynamic and sympathetic neural correlates of heart rate variability in congestive heart failure. Am J Cardiol. 1992; 69: 761–767. [Medline] [CrossRef]
13. Pomeranz B, Macaulay RJ, Caudill MA, Kutz I, Adam D, Gordon D, et al. Assessment of autonomic function in humans by heart rate spectral analysis. Am J Physiol. 1985; 248: H151–H153. [Medline]
14. Sun J, Deng G, Wang F, Mo J. Renal Hemodynamic Changes and Postsurgical Recovery in Children Treated for Ureteropelvic Junction Obstruction. Ultrasound Q. 2020; 36: 20–23. [Medline] [CrossRef]
15. Novellas R, Espada Y, Ruiz de Gopegui R. Doppler ultrasonographic estimation of renal and ocular resistive and pulsatility indices in normal dogs and cats. Vet Radiol Ultrasound. 2007; 48: 69–73. [Medline] [CrossRef]
16. Bragato N, Borges NC, Fioravanti MCS. B-mode and Doppler ultrasound of chronic kidney disease in dogs and cats. Vet Res Commun. 2017; 41: 307–315. [Medline] [CrossRef]
17. Freccero F, Petrucelli M, Cipone M, Nocera I, Sgorbini M. Doppler evaluation of renal resistivity index in healthy conscious horses and donkeys. PLoS One. 2020; 15: e0228741. [Medline] [CrossRef]
18. van de Kuit A, Benjamens S, Sotomayor CG, Rijkse E, Berger SP, Moers C, et al. Postoperative Ultrasound in Kidney Transplant Recipients: Association Between Intrarenal Resistance Index and Cardiovascular Events. Transplant Direct. 2020; 6: e581. [Medline] [CrossRef]
19. Olson MC, Abel EJ, Mankowski Gettle L. Contrast-Enhanced Ultrasound in Renal Imaging and Intervention. Curr Urol Rep. 2019; 20: 73–80. [Medline] [CrossRef]
20. Chang EH. An Introduction to Contrast-Enhanced Ultrasound for Nephrologists. Nephron. 2018; 138: 176–185. [Medline] [CrossRef]
21. Stock E, Vanderperren K, Bosmans T, Dobbeleir A, Duchateau L, Hesta M, et al. Evaluation of Feline Renal Perfusion with Contrast-Enhanced Ultrasonography and Scintigraphy. PLoS One. 2016; 11: e0164488. [Medline] [CrossRef]
22. Greenbarg EH, Jiménez DA, Nell LA, Schmiedt CW. Pilot study: use of contrast-enhanced ultrasonography in feline renal transplant recipients. J Feline Med Surg. 2018; 20: 393–398. [Medline] [CrossRef]
23. Komuro K, Seo Y, Yamamoto M, Sai S, Ishizu T, Shimazu K, et al. Assessment of renal perfusion impairment in a rat model of acute renal congestion using contrast-enhanced ultrasonography. Heart Vessels. 2018; 33: 434–440. [Medline] [CrossRef]
24. Stock E, Paepe D, Daminet S, Vandermeulen E, Duchateau L, Saunders JH, et al. Contrast-Enhanced Ultrasound Examination for the Assessment of Renal Perfusion in Cats with Chronic Kidney Disease. J Vet Intern Med. 2018; 32: 260–266. [Medline] [CrossRef]